Passive Seismic Characterization of Salt Jugs near William Street, South of the BNSF Railroad, and South of the Irsik & Doll Elevator in Hutchinson, KS

Shelby Peterie, Sarah Morton, Amanda Livers, Yuri Rupert, Brett Bennett,
Joe Anderson, Bryan Brooks, Joey Fontana, Brandon Graham,
Jeremy Scobee, Brett Wedel, Yao Wang, Julian Ivanov, and Richard Miller

Kansas Geological Survey
1930 Constant Avenue
Lawrence, KS 66047

Preliminary Report to

Alan J. Schmidt
Burns & McDonnell Engineering Company Inc.
1341 Opus Place, Suite 400
Downers Grove, IL 60515
(630) 724-3824

Open-file Report 2024-2 October 2015

Passive Seismic Characterization of Salt Jugs near William Street, South of the BNSF Railroad, and South of the Irsik & Doll Elevator in Hutchinson, KS

Executive Summary

This applied research project correlated measured shear-wave velocities with the characteristics of rock above dissolution voids, targeting the stress regime as approximated from the shear-wave velocity of the overburden. Shear-wave velocities were estimated during this study using passive surface-wave methods with data acquired over abandoned brine production wells along three profiles using train traffic as the uncontrolled source. Multichannel analysis of surface waves (MASW) was used to estimate the shear-wave velocity, loosely map stratigraphic contacts above the top of the dolomite unit well know as a shallow marker bed in this area ("three finger"), and to evaluate the relative difference in the rock above possible salt jugs associated with the wells compared to rocks above undisturbed salt. Five wells were targeted during seismic investigations in 2012 and 2015. Comparison of shear-wave velocity profiles over time (time lapse) was used to provide insight into void dynamics and overburden stability at wells where past data were acquired over these wells.

Passive MASW profiles were acquired during one night of data collection near the Irsik & Doll grain elevator, William Street, and south of the BNSF railroad in Hutchinson, Kansas, on June 22, 2015. A 2-D monitoring grid and three seismic lines were positioned over key wells. Continuous sampling was utilized to record and allow for evaluation of all available sources of passive source energy, ensuring optimal source orientation and surface-wave characteristics for each line. Surface waves with frequencies as low as 4 hertz (Hz) were recorded with an average depth of investigation of 55 meters (m), and in some places exceeding 60 m, successfully sampling around 20 m below the bedrock contact.

With shear-wave velocity being a function of shear modulus and density, and the shear modulus being the ratio of stress over strain, it is possible to estimate relative stress in overburden rocks (shear modulus) by measured shear velocity values. Local increases in shear velocity independent of lithology can reasonably be equated to increased stress in overburden roof load over dissolution jugs. Relative shear velocity lows may be associated with rock failure and collapse features whose vertical movement has been arrested by bulking, or changes in material properties due to natural variation in deposition or erosion.

Changes in dispersion patterns representative of subtle drops in sub-bedrock shear velocity at well 52 along the William Street line between October 2012 and June 2015 suggest some kind of incremental change has occurred above the old dissolution jug that may have reduced strength and/or redistributed stress in the overburden, such as a failure related to a vertically migrating void. This change in strength or stress appears to currently be confined to depths greater than 28 m below ground surface—approximately 18 m beneath the top of bedrock—and may have a lateral extent of up to 50 m, although this is uncertain and likely an overestimate. Shear velocity of bedrock at well 53, although elevated in the June 2015 survey, is consistent with the October 2012 survey. This suggests that the void at this well was stable during the time between surveys. A decrease in surface-wave penetration depths coincident with

well 7A (BNSF railroad line) may be related to a localized zone of reduced shear velocity at depths of 45 m or greater. This interpretation is relatively low-confidence and reduced surface-wave penetration likely represents natural geologic variation.

No significant increases or decreases in shear velocity were observed along the BNSF railroad line that intersects wells 7A and 4A or any wells sampled along William Street, with the exception of well 52 as noted previously. There appears to be no change above wells previously surveyed in the vicinity of the Irsik & Doll elevator and the first-time surveys over BNSF railroad proximity wells have no indications of elevated shear velocity relative to surrounding rock layers that exceed reasonable variations for this area.

Introduction

Material properties (specifically strength and stress accumulations) measured as a function of depth above abandoned salt jugs in Hutchinson, Kansas, appear related to the mobility and upward migration potential of these jugs. Localized escalation in stress (as indicated by increased shear-wave velocity) above subterranean voids is one indicator of an increased potential for roof failure and void migration (Eberhart-Phillips et al., 1989; Dvorkin et al., 1996; Khaksar et al., 1999; Sayers, 2004). Previous studies, using both active and passive seismic wavefield characteristics, suggest perturbations in the shear-wave velocity field immediately above voids can be correlated to characteristics of the unsupported roof spans of salt jugs in the Hutchinson area (Sloan et al., 2010).

The strength of individual rock layers can be qualitatively described in terms of stiffness/rigidity and empirically estimated from relative comparisons of shear-wave velocity measurements. Shear-wave velocity is directly proportional to stress and inversely related to non-elastic strain. Since the shear-wave velocity of earth materials changes when stress and any associated elastic strain on those materials becomes "large," it is reasonable to suggest load-bearing roof rock above mines or dissolution voids may experience elevated shear-wave velocities due to loading between pillars or, in the case of voids, loading between supporting side walls. This localized increase in shear velocity is not related to increased strength, but increased load as defined by Young's Modulus. High-velocity shear-wave "halos" encompassing low-velocity anomalies are suggested to be key indicators of near-term roof failure. All these phenomena have been observed within the overburden above voids in the Hutchinson Salt Member in Hutchinson at depths greater than 30 m below the bedrock surface.

Previous research projects at the Carey Boulevard Research Area (CBRA) correlated measured shear-wave velocities with the condition of dissolution voids and the physical properties of the overburden at selected locations on Vigindustries legacy solution mining property in Hutchinson. Shear-wave velocities were estimated from passive surface-wave data acquired along eight profiles that intersected 13 wells. Two of these 13 wells had been the target of a previous seismic investigation completed in 2008. As a result of that 2008 study it was determined that the integrity of the overlying strata could be reasonably estimated using shear-wave seismic imaging. The 2008 study quantified the effectiveness of shear-wave velocity to estimate local stress above voids of the size and depth prevalent at the Vigindustries site.

The lack of necessary ultra low-frequency surface waves in the recorded wavefield have negated attempts to use active source multi-channel analysis of surface waves (MASW) to estimate shear velocity in the lithified rocks near the top of bedrock (Miller et al., 2009). Uncontrolled, local industrial and transportation activities represent sound sources that have produced

the necessary low frequencies and, when recorded and processed using passive methods, have extended the imaging depth to over 60 m (Miller, 2011). Key to this method is the ability to estimate shear-wave velocities to depths more than double those possible with standard active sources at a particular site (Park et al., 2004). Results of passive MASW studies near this site suggest that this method is effective in identifying jugs with heightened risk for upward migration (Miller, 2011; Ivanov et al., 2013).

Wells 6B and 7B are located in relative proximity to the Irsik & Doll grain elevator. Seismic surveys were acquired over both wells in August 2012 and over 6B in October 2012. MASW processing resulted in three two-dimensional (2-D) shear-wave velocity (Vs) profiles. At the time of those surveys, 2-D Vs profiles above these wells suggested a normal stress regime with natural geologic variation. Wells 52, 53, and 59 are located near Williams Street. Active shear-wave reflection and passive surface-wave surveys were acquired over these wells in August 2008 and October 2012. In 2008, a decrease in shear-wave reflection stacking velocity and drop in coherency of bedrock and dolomite reflections at well 52 indicated reduced stress and possibly rock failure and collapse. Elevated Vs at well 53 suggested that a domed roof was gently distributing gradually increasing stress.

Individually, each seismic profile from a previous survey represents a snapshot in time that lacks any measure of the dynamics of void migration or change in time. In this study, an additional line was acquired over wells 6B, 7B, 52, 53, and 59 to monitor for and evaluate further changes in Vs, and provide insight into void dynamics and overburden stability. Baseline profiles acquired over wells 4A, 7A, and 60 will be used to estimate the shear-wave velocity, loosely map stratigraphic contacts above the top of the "three finger" dolomite, and evaluate the relative strength of the rock above possible salt jugs associated with these wells.

Geologic and Geophysical Setting

The Permian Hutchinson Salt Member occurs in central Kansas, northwestern Oklahoma, and the northeastern portion of the Texas Panhandle, and is prone to and has an extensive history of dissolution and formation of sinkholes (Figure 1). In Kansas, the Hutchinson Salt Member possesses an average net thickness of 75 m and reaches a maximum of over 150 m in the southern part of the basin. Deposition occurring during fluctuating sea levels caused numerous halite beds, 0.2 to 3 m thick, to be formed interbedded with shale, minor anhydrite, and dolomite/magnesite. Individual salt beds may be continuous for only a few miles despite the remarkable lateral continuity of the salt as a whole (Walters, 1978).

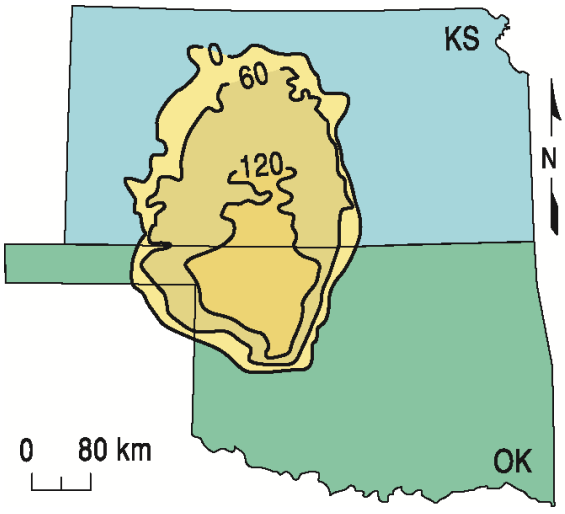

Figure 1. Approximate extent of salt formation, with contour intervals expressed in meters.

The distribution and stratigraphy of the salt is well documented (Dellwig, 1963; Holdoway, 1978; Kulstad, 1959; Merriam, 1963). The salt reaches a maximum thickness in central Oklahoma and thins to depositional edges on the north and west, erosional subcrop on the east, and facies changes on the south. The increasing thickness toward the center of the salt bed is due

to a combination of increased salt, and more and thicker interbedded anhydrites. The Stone Corral Formation (a well-documented seismic marker bed) overlies the salt throughout Kansas (McGuire and Miller, 1989). Directly above the salt at this site is a thick sequence of Permian shale.

The upper 760 m of rock at this site is Permian shale (Merriam, 1963). The Chase Group (top at 300 m deep), lower Wellington Shale (top at 245 m deep), Hutchinson Salt (top at 120 m deep), upper Wellington Shale (top at 75 m deep), and Ninnescah Shale (top at 25 m deep) make up the packets of reflecting events easily identifiable and segregated within the Permian portion of the section (Figure 2). Bedrock is defined as the top of the Ninnescah Shale with the sediment. The thickness of Quaternary alluvium that fills the stream valleys and paleo-subsidence features goes from 0 to as much as 90 m, depending on the dimensions of the features.

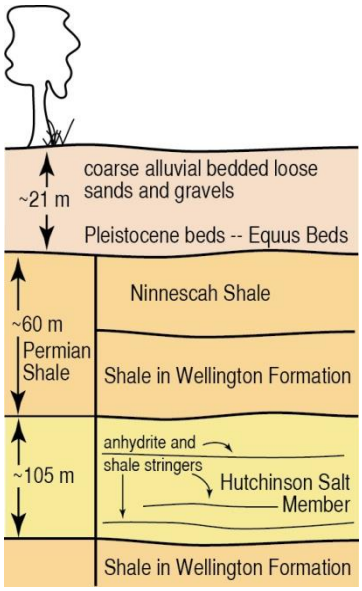

Figure 2. Generalized geology.

Recent dissolution of the salt and resulting subsidence of overlying sediments forming sinkholes has generally been associated with mining or saltwater disposal (Walters, 1978). Historically, these sinkholes can manifest themselves as a risk to surface infrastructure. The rate of surface subsidence can range from gradual to very rapid. Besides risks to surface structures, subsidence features potentially jeopardize the natural segregation of ground-water aquifers, greatly increasing their potential to negatively impact the environment (Whittemore, 1989; 1990). Natural sinkholes resulting from dissolution of the salt by localized leaching within natural flow systems which have been altered by structural features (such as faults and fractures) are not uncommon west of the main dissolution edge (Merriam and Mann, 1957).

Caprock and its characteristics are a very important component of any discussion concerning dissolution, subsidence, and formation of sinkholes. The Permian shales (Wellington and Ninnescah) that overlay the Hutchinson Salt Member are about 60 m thick in this area and are characterized as generally unstable when exposed to freshwater, being susceptible to sloughing and collapse (Swineford, 1955). These Permian shales tend to be red or reddish-brown and are commonly referred to as "red beds." Permian red beds are extremely impermeable to water and have provided an excellent seal between the freshwaters of the Equus beds and the extremely water-soluble Hutchinson Salt Member. The modern-day expanse and mere presence of the Hutchinson Salt is due to the protection from freshwater provided by these red beds.

Isolating the basal contact of the Wellington Formation provides key insights into the general strength of roof rock expected if dissolution-mined salt jugs (salt jugs are the jug-shaped cavities or voids in the salt that form after salt has been dissolution mined in proximity to the wells) reach the top of the salt zone. Directly above the salt/shale contact is approximately 6 m-thick dark-colored shale with joint and bedding cracks filled with red halite (Walters, 1978). Once unsaturated brine comes in contact with this shale layer, these red halite-filled joints and bedding planes are rapidly leached, leaving an extremely structurally weak layer.

Field Layout and Data Acquisition

To ensure the highest quality data, receivers were deployed during the day and train data were recorded at night when cultural and industrial noise was minimal to provide optimum signal-to-noise. Analysis of the previous seismic energy sources captured during passive recording at this site clearly indicated trains from a distance of 3 kilometers (km) or more away provided the best broad spectrum, low-frequency seismic energy (Miller, 2011). Because seismic energy with characteristics best suited for the purpose of this study may arrive when trains are at a distance greater than they can be detected by spotters, seismic records were recorded continuously during acquisition to ensure that optimum data was recorded.

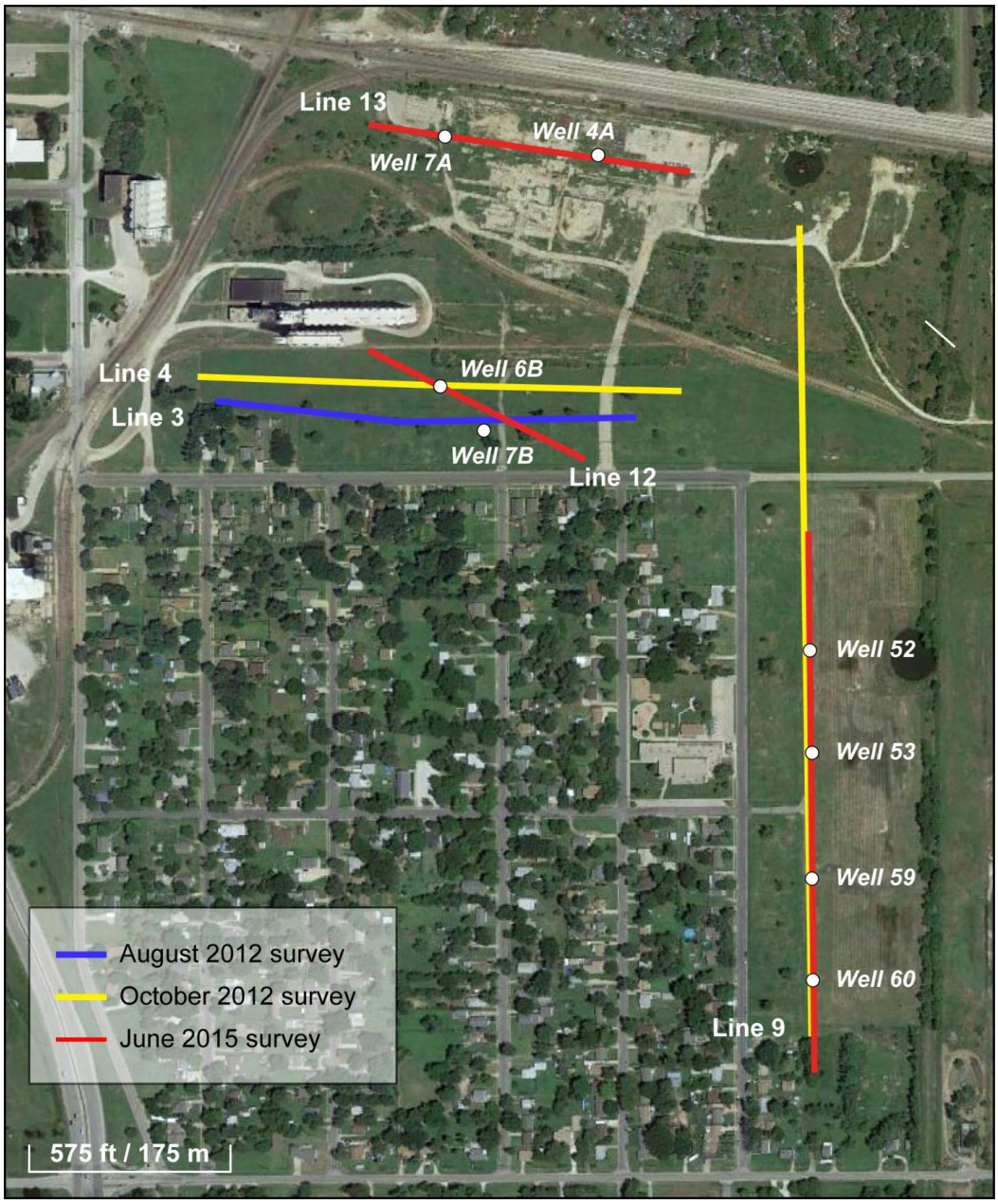

Figure 3. Aerial photo with GPS locations of seismic lines and wells in the study area.

Data were acquired over the course on the night of June 22, 2015. A total of three seismic lines were deployed over key wells, as well as a 2-D grid of receivers to monitor passive seismic energy (Figure 3). Seismic receivers were single GeoSpace GS-11D 4.5 Hz geophones spaced at 3 m intervals. The seismic lines totaled approximately 1 km in length. The 2-D monitoring grid consisted of 144 receivers spaced at 5 m intervals and was configured to form four concentric expanding squares with 10, 30, 50, and 70 m sides. Data were recorded during one night with a 350+ channel 24-bit Geometrics Geode distributed seismic system. Seismic records were 30 seconds (s) long with a 2 millisecond (ms) sampling interval. In total, 586 seismic records equivalent to 15.1 gigabytes (GB) of data were recorded.

Processing and Analysis

Data were processed using algorithms developed at the Kansas Geological Survey (KGS). The passive method used for this study is well published and provides good quality results at a similar nearby site (Park et al., 2004; Ivanov et al., 2013). Continuous data acquisition records energy from nearby energy sources at various orientations with respect to the seismic line. The 2-D grid was deployed to evaluate and optimize source alignment with respect to each 1-D seismic line to effectively identify void roofs with elevated stress and an elevated risk of vertical migration.

For each line, the surface-wave amplitudes recorded by the 2-D grid were plotted as phase velocity versus frequency for a range of azimuths from 0 to 360 degrees with respect to the seismic line to determine which record had the best broad band, low frequency source with an azimuth near parallel to the line (Figure 4). The seismogram with optimum source characteristics was selected and divided into the shortest groups of receivers ("spread length") which provided dispersion patterns on phase velocity versus frequency plots with high amplitude fundamental-mode Rayleigh-wave energy and minimal higher-order surface-wave interference (Figure 5). Due to a change in the inversion algorithm, data from the Fundamental mode dispersion curves were picked and inverted to obtain a 2-D section of shear-wave velocity as a function of depth. The apparent velocity (v_{app}) is:

$$v_{app} = \frac{v_{act}}{(\cos\theta)} \tag{1}$$

where v_{act} is the actual seismic velocity and θ is the azimuth of the source with respect to the seismic line determined from the azimuth versus frequency plot. Thus, the increase in velocity (Δv) is:

$$\Delta v = \frac{1}{\cos\theta} - 1 \tag{2}$$

Equation 2 was used to calculate the increase in velocity due to the source azimuth for each line (Table 1).

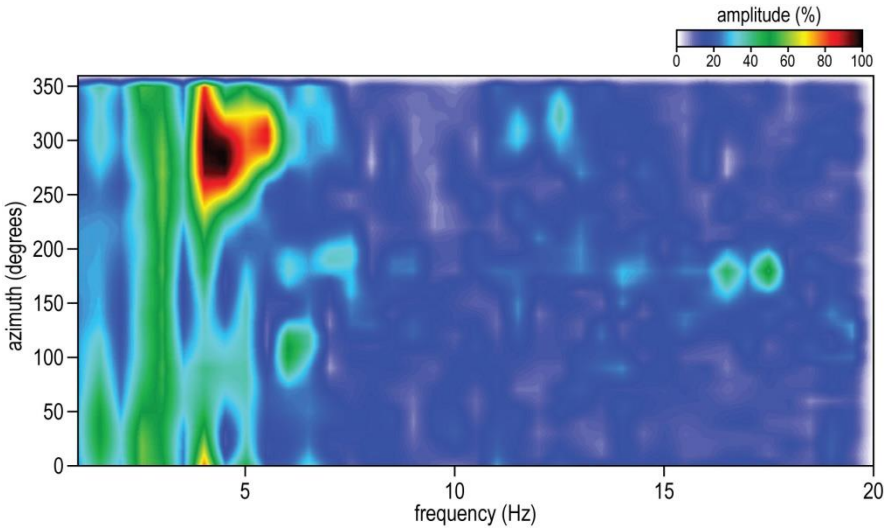

Figure 4. Azimuth plot indicating the direction of the dominant passive source energy (in degrees counter-clockwise from east). Here, the dominant passive source energy is centered on approximately 290°.

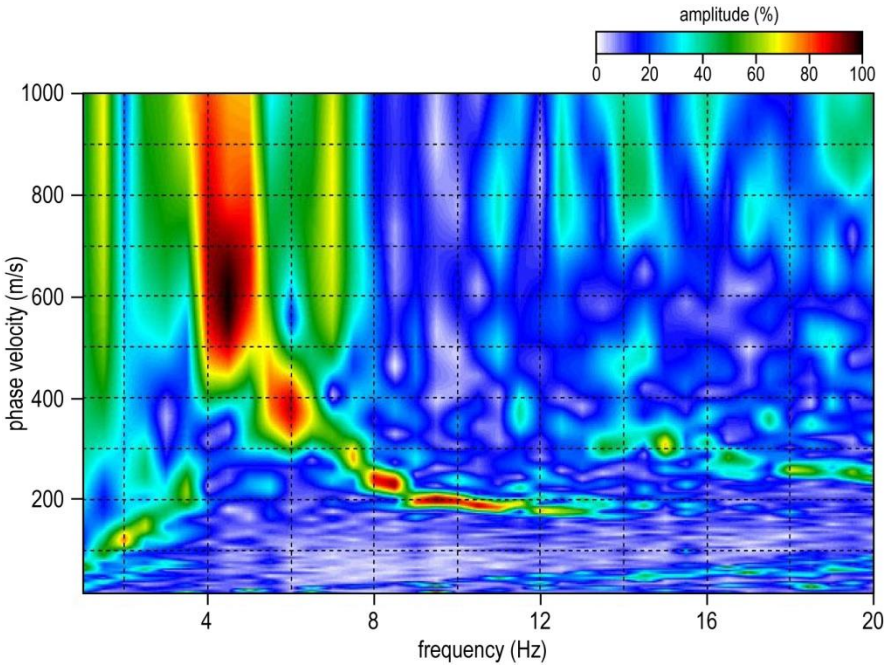

Figure 5. Dispersion pattern with high signal-to-noise ratio of the fundamental mode Rayleigh wave.

Table 1. Directions of the passive seismic sources and the seismic lines (in degrees counterclockwise from east), the angle of the source with respect to the line (θ), and the percent increase in apparent velocity (Δv) attributable to oblique source orientations.

	source orientation	line orientation	θ	Δv
line 9	270°	290°	20°	6 %
line 12	159°	152°	7°	< 1%
line 13	180°	174°	6°	< 1%

Results and Observations

Line 9 is oriented north-south along William Street. Top of bedrock is at a depth of approximately 10-15m (Figure 6a). Velocities observed in the June 2015 2-D Vs profile (Figure 6a) are as a whole ~20% lower than observed in October 2012 (Figure 6b) and the October 2012 results have a smoother appearance. Characteristics of the passive seismic sources are, by nature, variable and uncontrollable. The optimal source for one survey may have different characteristics than another survey. Therefore, each survey was processed using parameters that generate optimal dispersion patterns, which vary from survey to survey.

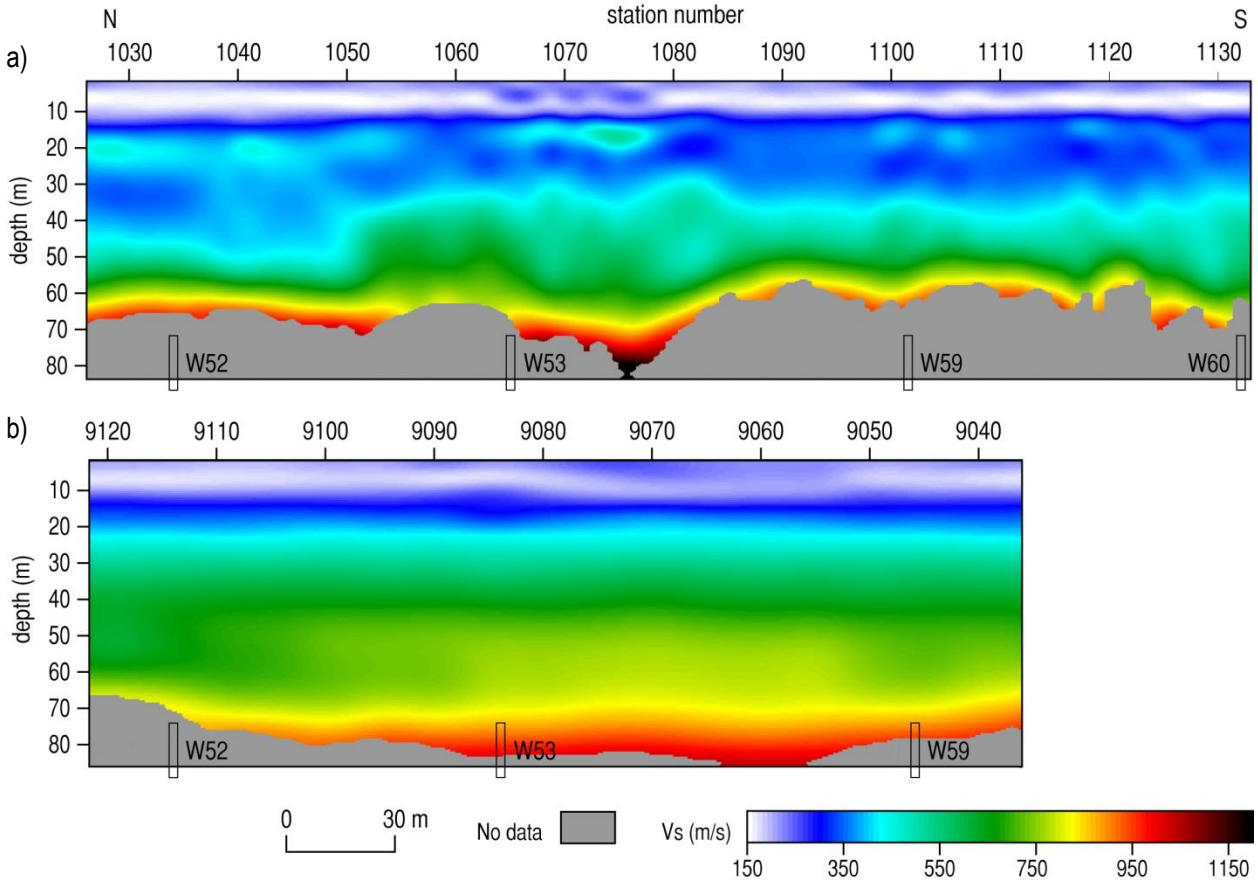

Figure 6. Shear-wave velocity profile of line 9 from (a) June 2015, and (b) October 2012. Approximate well locations are indicated at the bottom of the profiles.

To improve the signal-to-noise ratio and coherency of dispersion curves in October 2012, multiple time windows were stacked to attenuate passive noise from azimuths that were not aligned with the seismic line. The tradeoff is some degree of smearing of dispersion patterns, which may result in a small systematic increase in apparent shear velocity. The ~20% greater velocities observed in October 2012 is likely, at least in part, a result of stacking time windows to improve signal-to-noise. Additionally, due to the higher signal-to-noise ratio in June 2015, these data were processed with a shorter spread length, which, combined with denser spatial sampling, improved horizontal resolution.

The shear velocity profiles from line 9 of the current survey and the October 2012 study are generally consistent. Reduced bedrock velocity is observed at well 52 and elevated velocity observed at well 53. Bedrock velocity around wells 59 and 60 represent natural geologic variation. For a more direct time-lapse comparison, dispersion patterns from October 2012 were re-generated using the same processing parameters used to generate the June 2015 dispersion patterns. Dispersion curves from June 2015 are superimposed on dispersion patterns from October 2012 to make relative comparisons at select locations on line 9.

Due to relatively poor resolution of the fundamental mode Rayleigh wave in October 2012 (Figure 7b), it is difficult to interpret the dispersion curve at well 52 with high confidence. However, the dominant signal from 4-7 Hz has a faster Rayleigh wave phase velocity than the fundamental mode dispersion curve observed at this location in 2015 (Figure 7). This suggests a real decrease in shear velocity at well 52 at depths of approximately 28 m and greater. The 2-D Vs profile from June 2015 indicates that the reduced velocity zone may extend as far as station 1051 (Figure 6a), 50 m south of well 52. Dispersion patterns at this location do suggest a slight reduction in velocity in the 2.5 years between surveys (Figure 8). At and near well 53, the dispersion patterns observed in June 2015 are consistent with the dispersion patterns from October 2012 (Figure 9), suggesting no significant changes in the subsurface at this well.

Line 12 is oriented approximately northwest-southeast and is located southeast of the Irsik & Doll grain elevator. Top of bedrock is at a depth of approximately 10-15 m (Figure 10a). Similar to line 9, the data acquired in 2012 have slightly higher velocities (Figure 10b). In general, the velocity profile from June 2015 is consistent with the profiles acquired over these wells in 2012 and suggests natural geologic variation.

Line 13 is oriented approximately west-east and is located ~60 m south of the BNSF railroad. Top of bedrock is at a depth of approximately 10 m (Figure 11). Bedrock velocity is 450 m/s on average and in general represents natural geologic variation. Depth of surface-wave penetration is slightly reduced at well 7A with a ~2 m increase in the depth to bedrock. Dispersion patterns from stations 3022-3030 indicate a consistent velocity at 8 Hz (Figure 12), which corresponds to approximately the top of bedrock. Therefore, the apparent variability in the top of bedrock is not real and likely an artifact of inversion, related to a decrease in the surface-wave penetration within this zone. Dispersion patterns suggest that the decrease in depth of penetration may be the result of a localized decrease in velocity at stations 3022-3025.

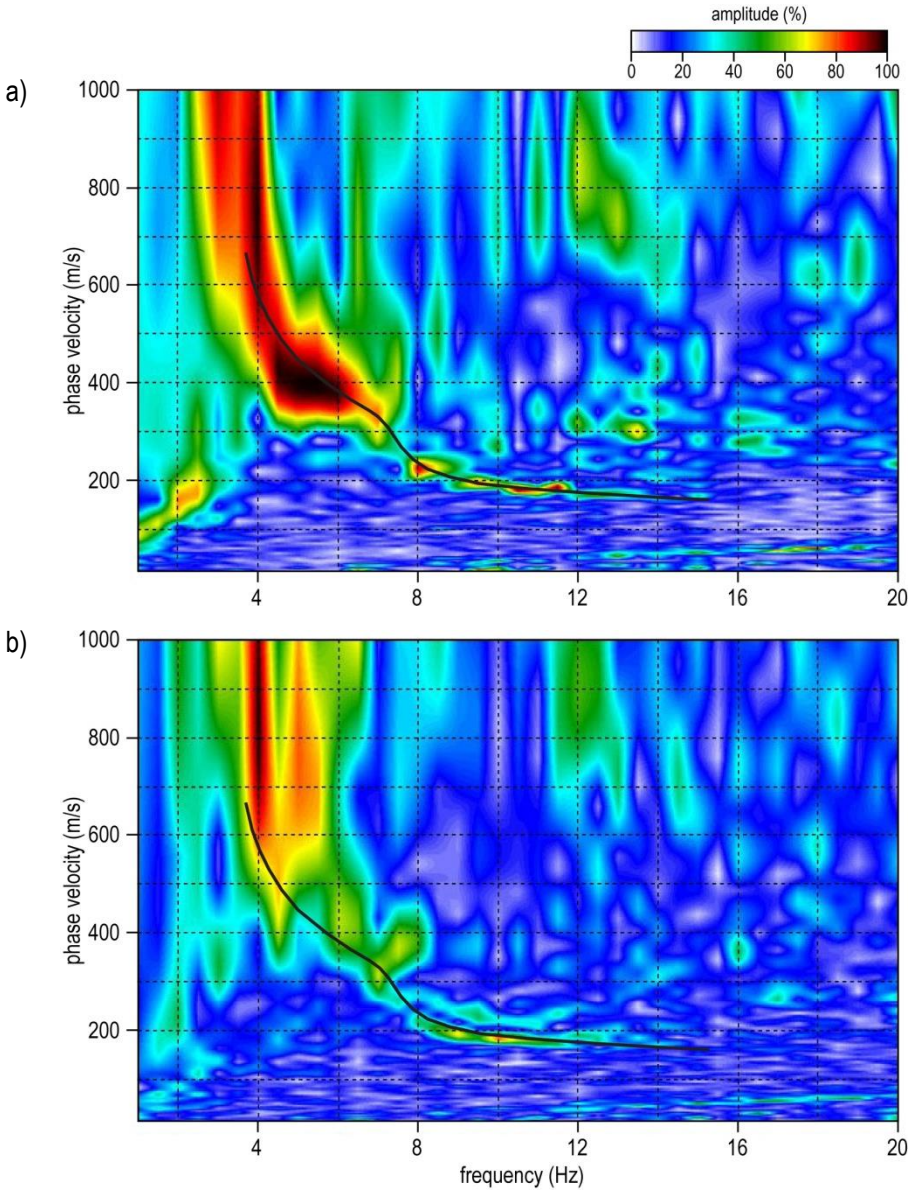

Figure 7. Dispersion patterns at well 52 from (a) June 2015 and (b) October 2012. Black line represents the June 2015 dispersion curve.

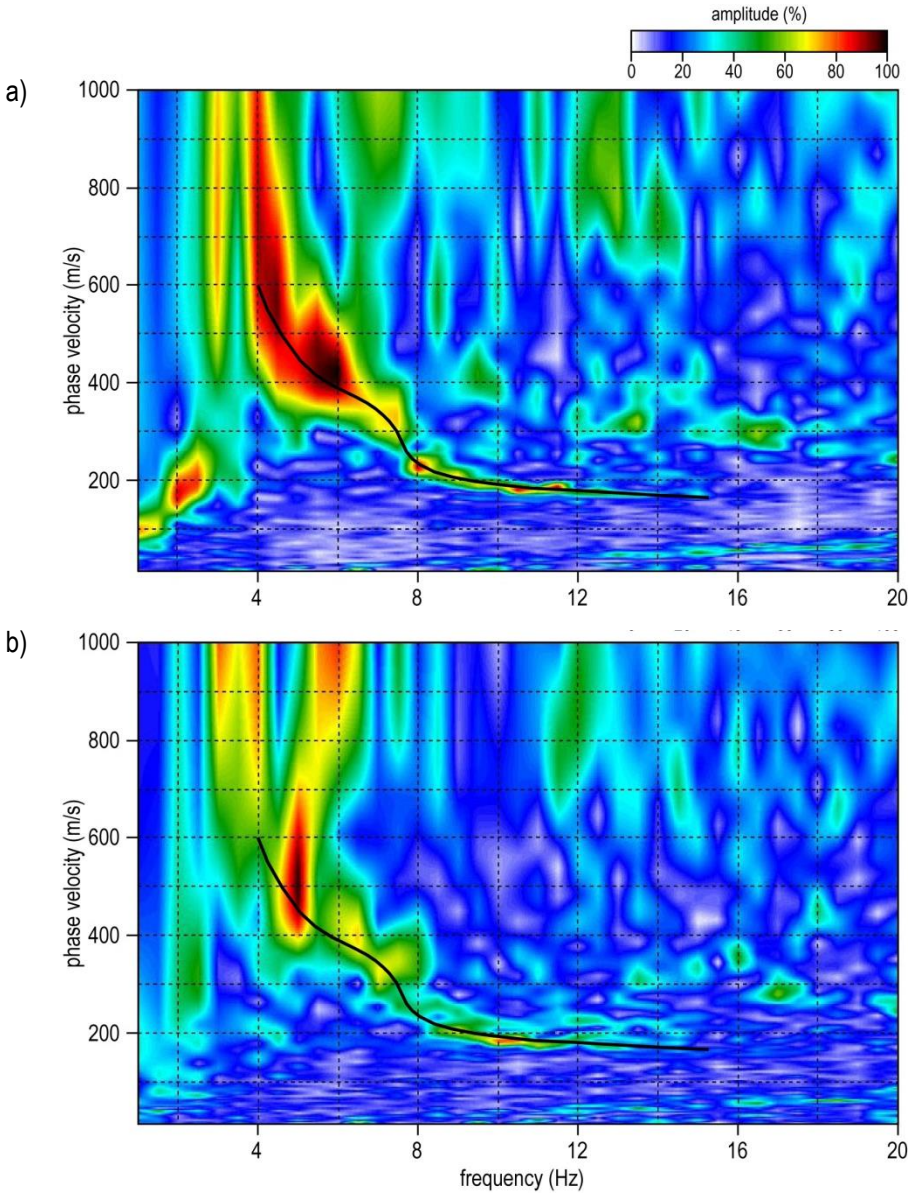

Figure 8. Dispersion patterns 48 m south of well 52 (a) at station 1052 in June 2015 and (b) the equivalent location in October 2012. Black line represents the June 2015 dispersion curve.

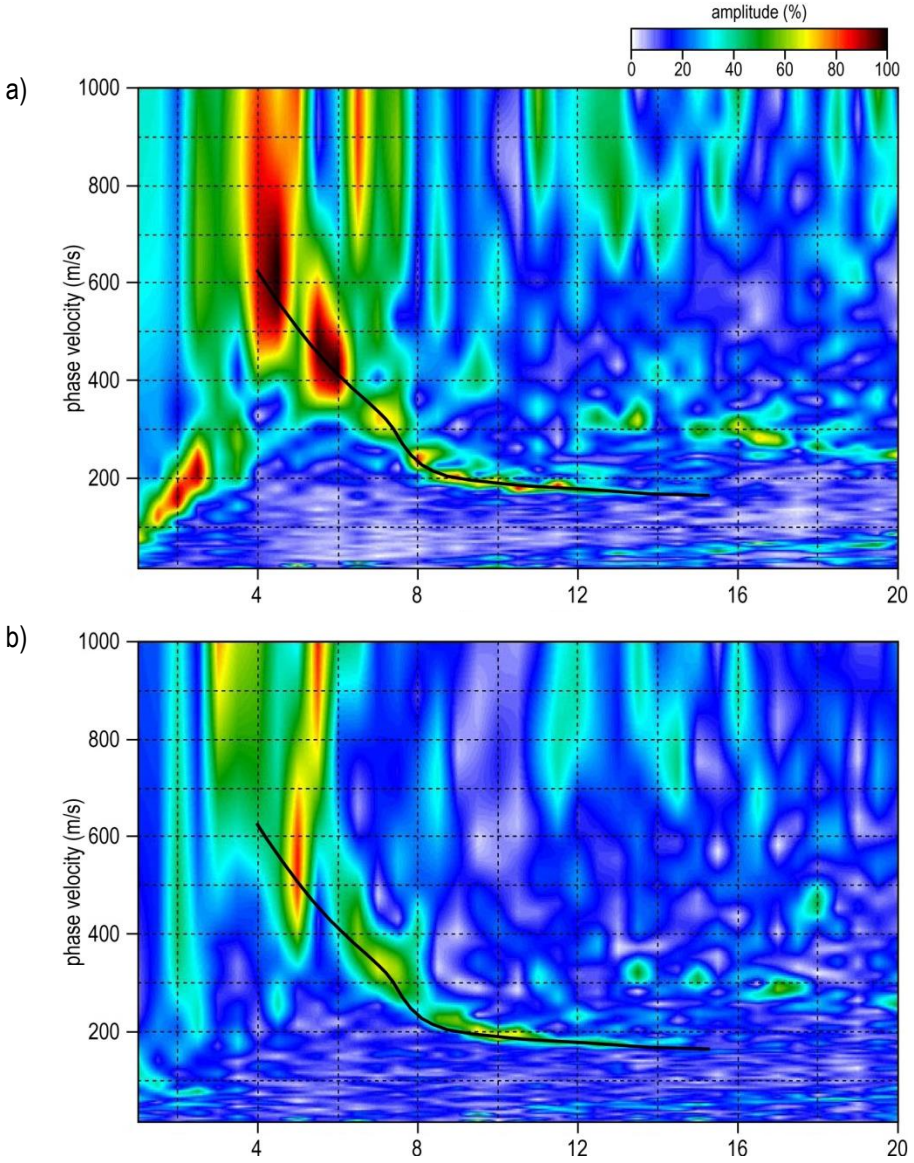

Figure 9. Dispersion patterns at well 53 from (a) June 2015 and (b) October 2012. Black line represents the June 2015 dispersion curve.

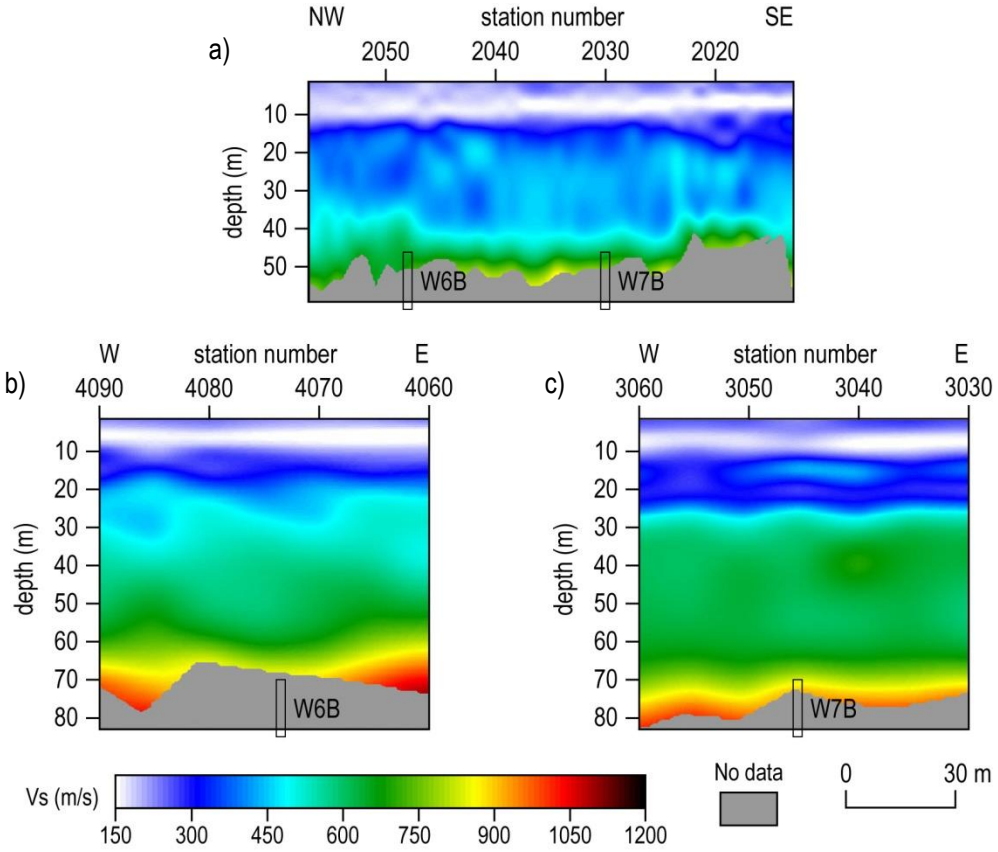

Figure 10. Shear-wave velocity profile of (a) line 12 from June 2015, (b) well 6B extracted from line 4 acquired in October 2012, and (c) well 7B extracted from line 3 acquired in August 2012. Approximate well locations are indicated at the bottom of the profiles.

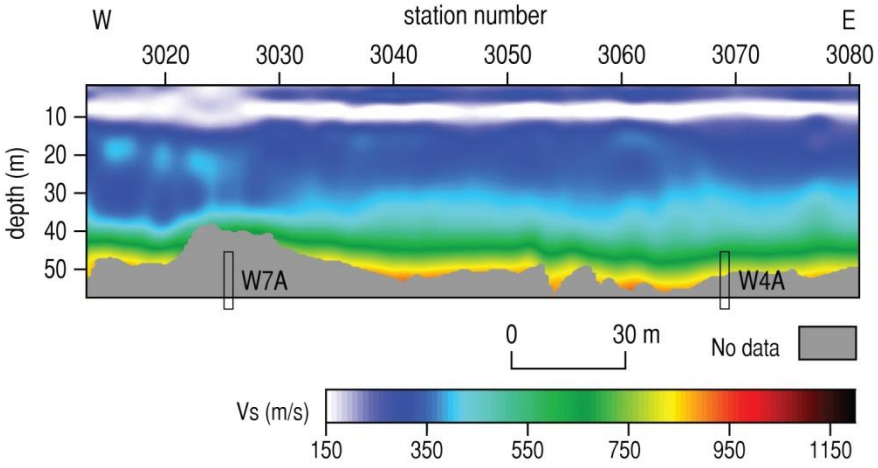

Figure 11. Shear-wave velocity profile from line 13 of the June 2015 survey. Approximate well locations are indicated at the bottom of the profiles.

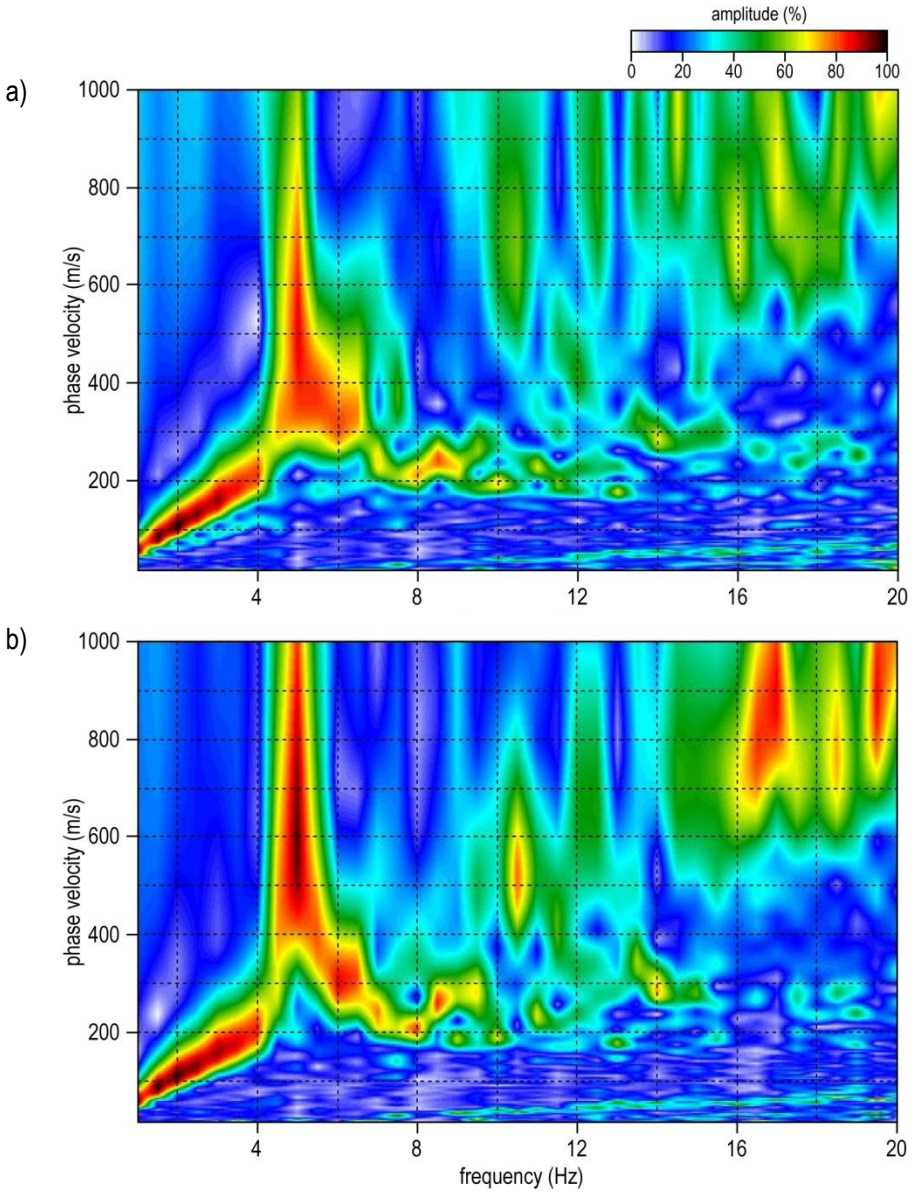

Figure 12. Dispersion pattern from line 13 at (a) well 7A and (b) station 3035.

Interpretation and Discussion

Wells 52 and 53

Due to variability in source characteristics, signal-to-noise ratio, and different processing parameters required for optimal dispersion analysis of line 9 along Williams Street, the Vs profiles cannot be directly compared. Dispersion patterns computed with the same parameters provide more accurate relative comparisons and insight into time-lapse changes in the shear strength of the subsurface. At well 52, dispersion patterns indicate reduced surface-wave phase velocity in June 2015 relative to October 2012 (Figures 7 and 8). This suggests a change in material properties consistent with continued incremental failure in the bedrock overlying the void at this well. This does not necessarily imply that the roof of the void has physically collapsed, but that some kind of failure may have reduced strength in the overburden and/or redistributed stress within bedrock. Changes in dispersion patterns at and near well 52 suggest that failure was limited to depths greater than 28 m, but may have a lateral extent up to 50 m from the well. However, the spread size used to generate optimal dispersion patterns was 150 m. This large spread size results in horizontal averaging; thus, the lateral extent of the reduced velocity zone is uncertain and may be smaller.

Elevated bedrock velocity at well 53 was observed in both October 2012 and June 2015 (Figure 6). Surface waves recorded at this well during the two surveys have very similar dispersion patterns (Figure 9), indicating that little if any change has occurred in the overall stress regime at this well at the time of the surveys. It is possible that periodic episodes of incremental failure and buildup of stress have occurred in the interim. Lack of significant observable change suggests that, although the bedrock above this void continues to exhibit elevated velocity, the void is likely relatively stable with low immediate risk of vertical migration.

Well 7A

A decrease in surface-wave penetration depth is observed near well 7A. Dispersion patterns suggest that the decrease in depth of penetration may be the result of a localized decrease in velocity at stations 3022-3025 (Figure 12a). However, the resolution of the fundamental mode dispersion pattern is lower at these locations relative to the rest of line 13 (e.g., Figure 12b); the true phase velocity may be higher and consistent with adjacent stations. Although variability in surface-wave penetration depth is not necessarily anomalous in and of itself, its coincidental location with well 7A suggests the possibility of reduced bedrock strength at a depth of 45 m. However, confidence in this interpretation is relatively low.

Wells 4A, 6B, 7B, 59, 60

Velocity profiles over these wells are representative of natural geologic variation and a normal stress regime.

Conclusions

Subtle drops in sub-bedrock velocity at well 52 between October 2012 and June 2015 suggest some kind of incremental change has occurred above the old dissolution jug that may have reduced strength and/or redistributed stress in the overburden. This change in strength or stress appears to currently be confined to depths greater than 28 m below ground surface—approximately 18 m beneath the top of bedrock—and may have a lateral extend of up to 50 m,

although this is uncertain and likely an overestimate. No significant time-lapse changes occurred since 2012 at wells 53, 59, 6B, or 7B. Bedrock velocity at well 53 was elevated in both June 2015 and October 2012. Dispersion patterns indicate no significant change in velocity, suggesting a stable void during the time since the previous survey. Velocity profiles acquired in June 2015 over wells 4A and 60 suggest natural geologic variation and a normal stress regime. A decrease in surface-wave penetration depths coincident with well 7A may be related to a localized zone of reduced velocity at depths of 45 m or greater. This interpretation is relatively low-confidence and reduced surface-wave penetration likely represents natural geologic variation.

References

Dellwig, L.F., 1963, Environment and mechanics of deposition of the Permian Hutchinson Salt Member of the Wellington shale: Symposium on Salt, Northern Ohio Geological Society, p. 74-85.

Dvorkin, J., A. Nur, and C. Chaika, 1996, Stress sensitivity of sandstones: *Geophysics*, v. 61, p. 444-455.

Eberhart-Phillips, D., D.-H. Han, and M.D. Zoback, 1989, Empirical relationships among seismic velocity, effective pressure, porosity, and clay content in sandstone: *Geophysics*, v. 54, p. 82-89.

Holdoway, K.A., 1978, Deposition of evaporites and red beds of the Nippewalla Group, Permian, western Kansas: Kansas Geological Survey Bulletin 215.

Ivanov, J., R.D. Miller, S.L. Peterie, J.T. Schwenk, J.J. Nolan, B. Bennett, B. Wedel, J. Anderson, J. Chandler, and S. Green, 2013, Enhanced passive seismic characterization of high priority salt jugs in Hutchinson, Kansas: Preliminary report to Burns & McDonnell Engineering Company.

Khaksar, A., C.M. Griffiths, and C. McCann, 1999, Compressional- and shear-wave velocities as a function of confining stress in dry sandstones: *Geophysical Prospecting*, v. 47, p. 487-508.

Kulstad, R.O., 1959, Thickness and salt percentage of the Hutchinson salt; *in* Symposium on Geophysics in Kansas: Kansas Geological Survey Bulletin 137, p. 241-247.

McGuire, D., and B. Miller, 1989, The utility of single-point seismic data; *in* Geophysics in Kansas, D.W. Steeples, ed.: Kansas Geological Survey Bulletin 226, p. 1-8.

Merriam, D.F., 1963, The Geologic History of Kansas: Kansas Geological Survey Bulletin 162, 317 p.

Merriam, D.F., and C.J. Mann, 1957, Sinkholes and related geologic features in Kansas: *Transactions of the Kansas Academy of Science*, v. 60, p. 207-243.

Miller, R.D., 2011, Progress report: 3-D passive surface-wave investigation of solution mining voids in Hutchinson, Kansas: Interim report to Burns & McDonnell Engineering Company, January, 9 p.

Miller, R.D., J. Ivanov, S.D. Sloan, S.L. Walters, B. Leitner, A. Rech, B.A. Wedel, A.R. Wedel, J.M. Anderson, O.M. Metheny, and J.C. Schwarzer, 2009, Shear-wave study above Vig-industries, Inc. legacy salt jugs in Hutchinson, Kansas: Kansas Geological Survey Open-file Report 2009-3.

Park, C., R. Miller, D. Laflen, N. Cabrillo, J. Ivanov, B. Bennett, and R. Huggins, 2004, Imaging dispersion curves of passive surface waves [Exp. Abs.]: Annual Meeting of the Soc. of Expl. Geophys., Denver, Colorado, October 10-15, p. 1357-1360.

Sayers, C.M., 2004, Monitoring production-induced stress changes using seismic waves [Exp. Abs.]: Annual Meeting of the Soc. of Expl. Geophys., Denver, Colorado, October 10-15, p. 2287-2290.

Sloan, S.D., S.L. Peterie, J. Ivanov, R.D. Miller, and J.R. McKenna, 2010, Void detection using near-surface seismic methods; *in* Advances in Near-Surface Seismology and Ground-Penetrating Radar, SEG Geophysical Developments Series No. 15, R.D. Miller, J.D. Bradford, and K. Holliger, eds.: Tulsa, Society of Exploration Geophysicists, p. 201-218.

Swineford, A., 1955, Petrography of upper Permian rocks in south-central Kansas: State Geological Survey of Kansas Bulletin 111, 179 p.

Walters, R.F., 1978, Land subsidence in central Kansas related to salt dissolution: Kansas Geological Survey Bulletin 214, 82 p.

Whittemore, D.O., 1990, Geochemical identification of saltwater contamination at the Siefkes subsidence site: Report for the Kansas Corporation Commission.

Whittemore, D.O., 1989, Geochemical characterization of saltwater contamination in the Macksville sink and adjacent aquifer: Kansas Geological Survey Open-file Report 89-35.